# Neutrino oscillations and moments of electron spectra

J. N. Bahcall and P. I. Krastev

*Institute for Advanced Study, Princeton, New Jersey 08540*

E. Lisi

*Institute for Advanced Study, Princeton, New Jersey 08540 and Dipartimento di Fisica and Sezione INFN di Bari, 70126 Bari, Italy*

(Received 18 July 1996)

We show that the effects of neutrino oscillations on $^8$B solar neutrinos are described well by the first two moments (the average and the variance) of the energy distribution of scattered or recoil electrons. For the SuperKamiokande and the Sudbury Neutrino Observatory experiments, the differences between the moments calculated with oscillations and the standard, no-oscillation moments are greater than three standard deviations for a significant fraction of the neutrino mass-mixing ($\Delta m^2$, $\sin^2 2\theta$) parameter space. [S0556-2813(97)03901-0]

PACS number(s): 26.65.+t, 14.60.Pq, 13.15.+g

## I. INTRODUCTION

A full Monte Carlo simulation is necessary in order to understand in detail the results of complicated experiments and to estimate their uncertainties. Extensive simulations will be especially important for the next generation of solar neutrino experiments [1] in which background effects, energy-dependent sensitivities, and crucial geometrical factors will influence the measured rates. Experimentalists will have the time and patience to test a finite set of hypotheses against the results of their measurements and massive simulations and will report the results to an eagerly-waiting community of physicists and astronomers.

What additional information will be most useful to report?

We focus here on the crucial tests of the *shape* of the continuum neutrino spectrum, which are independent of solar physics to a fractional accuracy of $\mathcal{O}(10^{-5})$ [2]. Distortions of the energy spectra of neutrino-induced electrons could indicate neutrino oscillations.

We show in this paper that the first two moments of the (recoil or scattering) electron energy distribution—the average energy and the variance of the spectrum—can provide a compact and informative summary of the expected effects of neutrino oscillations on the continuum solar neutrino spectra. It is more practical to report the first two moments of the electron energy distribution and their uncertainties than to describe in detail the output of an extensive Monte Carlo simulation. Moreover, theorists can conveniently use the measured values of the average kinetic energy and its dispersion, instead of a binned energy spectrum, to test different models of neutrino interactions.

We calculate the changes in the first two spectrum moments, that are caused by vacuum neutrino oscillations and by matter-enhanced oscillations, in the two-flavor approximation. We illustrate our results by realistic numerical studies of the SuperKamiokande [3] (electron-neutrino scattering) and the Sudbury Neutrino Observatory [4] (SNO, neutrino absorption) detectors.

The structure of our paper is the following. In Sec. II we discuss the basic characteristics of the SuperKamiokande and SNO experiments, and present the standard (i.e., no oscilla-

tion) expectations for the average kinetic energy, $\langle T \rangle$, and the variance of the energy distribution, $\sigma^2$. In Sec. III we describe our calculation of the spectral moments in the presence of neutrino oscillations. In Sec. IV we show the results in the neutrino mass-mixing plane. In Sec. V we estimate realistic uncertainties. In Sec. VI we show how SuperKamiokande and SNO can discriminate new physics in representative cases. We summarize our work in Sec. VII.

We recall that the SNO experiment will, in addition to the electron spectrum shape meaurement, determine the ratio of the charged-to-neutral current interactions of neutrinos in deuterium, which is a powerful indicator of neutrino oscillations [5]. This measurement has been investigated in several papers (see the recent works [6–8]) and is not considered here.

## II. BASICS AND STANDARD PREDICTIONS

In this section we discuss the basic characteristics of the SNO and SuperKamiokande experiments, and calculate the standard electron energy spectra[1] expected in the absence of oscillations. We also evaluate the standard values of the first two moments of the electron energy spectra for SNO and SuperKamiokande. We discuss how well the two-moment approximation can parametrize the deviations from the standard electron spectra.

### A. Experimental characteristics

The SNO experiment [4] makes use of a 1 kt heavy-water Cherenkov detector [9] to observe the charged current (CC) neutrino-deuterium reaction:

$$\nu_e + d \rightarrow p + p + e^-. \tag{1}$$

The electron kinetic energy, $T$, is distributed between 0 and $E_\nu - Q$, where $E_\nu$ is the neutrino energy and $Q = 1.442$ MeV. The differential cross section for this reaction has been

---

[1]The standard electron energy spectrum at SNO has also been discussed in detail in [8].

TABLE I. Electron energy threshold and resolution parameters adopted in the analysis. Uncertainties are at $1\sigma$.

| Detector parameter | Symbol | SuperKamiokande | SNO |
|---|---|---|---|
| Kinetic energy threshold | $T_{\min}$ | 5 MeV | 5 MeV |
| Resolution width at 10 MeV | $\Delta_{10}$ | $1.6(1\pm0.01)$ MeV | $1.1(1\pm0.10)$ MeV |
| Energy scale uncertainty | $\delta$ | $\pm 100$ keV | $\pm 100$ keV |

recently discussed in detail in [8], to which the reader is referred for specific results and additional references [10].

The SuperKamiokande experiment [3] makes use of a 22 kt (fiducial volume) water-Cherenkov detector [11] to observe neutrino-electron scattering. The basic reaction is

$$\nu_e + e^- \rightarrow \nu_e' + e^-, \qquad (2)$$

in which both charged currents (CC) and neutral currents (NC) contribute. The electron kinetic energy $T$ is distributed almost uniformly between 0 and $E_\nu/(1+2m_e/E_\nu)$. The cross section is known to first order in the radiative corrections [12,10].

If neutrino oscillations $\nu_e \leftrightarrow \nu_x$ to an active neutrino occur, the pure NC reaction $\nu_x$-$e$ also contributes to the SuperKamiokande signal:

$$\nu_x + e^- \rightarrow \nu_x' + e^- \quad (x=\mu,\tau). \qquad (3)$$

In the following, we assume $x=\mu$ for definiteness.

If the SuperKamiokande and SNO detectors work as expected, high signal-to-noise ratios will be achieved above a threshold energy $T_{\min}\simeq5$ MeV. The background assessment is one of the most difficult aspects of these experiments. In the absence of reliable knowledge of the background, we make the optimistic assumption that there is no significant background contamination above a nominal 5 MeV threshold for both experiments. We also assume that the detection efficiency is constant above threshold.

The electron kinetic energy (and direction) will be measured, in both experiments, by the Cherenkov light. The distribution of the measured kinetic energy $T$ around the *true* kinetic energy $T'$ can be described by an energy resolution function of the form

$$R(T,T') = \frac{1}{\Delta_{T'}\sqrt{2\pi}}\exp\left[-\frac{(T'-T+\delta)^2}{2\Delta_{T'}^2}\right]. \qquad (4)$$

In Eq. (4), the bias term $\delta$ accounts for a possible uncertainty in the absolute energy calibration, and the energy-dependent one-sigma width $\Delta_{T'}$ scales as $\sqrt{T'}$ due to the photon statistics:

TABLE II. Standard predictions for the average kinetic energy, $\langle T \rangle$, and for the variance, $\sigma^2$, of the electron spectra at SuperKamiokande and SNO in the absence of oscillations.

| Experiment | $\langle T \rangle_0$ (MeV) | $\sigma_0^2$ (MeV$^2$) |
|---|---|---|
| Super Kamiokande | 7.296 | 3.42 |
| SNO | 7.658 | 3.04 |

$$\Delta_{T'} = \Delta_{10}\sqrt{T'/(10\text{ MeV})}, \qquad (5)$$

where $\Delta_{10}$ is the energy resolution width at 10 MeV.

The reference parameters $T_{\min}$, $\delta$, and $\Delta_{10}$ used in this work for SuperKamiokande [13] and SNO [14] are given in Table I. In SuperKamiokande, the energy resolution width $\Delta_{10}$ is expected to be measured with 1% accuracy by means of a dedicated, high statistics calibration with a tunable linear electron accelerator [13].

### B. Standard expectations

We have calculated the standard (i.e, no oscillation) electron spectra in SuperKamiokande and SNO, using the detector parameters given in Table I, the best-estimate cross sections for the reactions in Eq. (1) [15,8] and Eq. (2) [12], and the standard $^8$B neutrino spectrum [16].

Table II gives the calculated values of the first two spectral moments of the standard distributions, the average electron kinetic $\langle T \rangle_0$ and the variance $\sigma_0^2$.

Figure 1 compares the normalized standard spectrum (area = 1, solid line labeled STD) with three representative spectra calculated assuming neutrino oscillations in vacuum [17] or oscillations enhanced by the Mikheyev-Smirnov-Wolfenstein (MSW) effect [18] in the sun.[2] The spectra with oscillations refer to the values of the neutrino mass-mixing parameters $\Delta m^2$ and $\sin^2 2\theta$ that best-fit [7] the small-angle MSW (SMA), the large-angle MSW (LMA), and the vacuum oscillation (VAC) solutions[3] to the solar neutrino problem, given the published results of the four pioneering solar neutrino experiments [19–22].

The LMA solution does not induce any appreciable difference from the standard spectrum, since the corresponding electron survival probability, $P(E_\nu)=P(\nu_e\rightarrow\nu_e|E_\nu)$, is almost constant for $E_\nu\gtrsim5$ MeV. Hence the LMA spectrum is almost indistinguishable from the standard spectrum in Figs. 1(a) and 1(b). However, for the SMA and especially for the VAC cases illustrated, there are significant spectral distortions with respect to the no-oscillation (STD) case. The deviations in the spectral moments, $\langle T \rangle - \langle T \rangle_0$ and $\sigma^2 - \sigma_0^2$, are discussed in Sec. IV.

### C. Two-moment approximation

In this section we discuss the extent to which the deviations of the first two moments characterize the deformations of the electron spectrum induced by neutrino oscillations.

---

[2]The MSW regeneration of $\nu_e$ in the earth is not included in the present work.

[3]The best-fit values $(\Delta m^2, \sin^2 2\theta)$ for the SMA, LMA, and VAC cases are respectively $(5.4\times10^{-6}$ eV$^2$, $7.9\times10^{-3})$, $(1.7\times10^{-5}$ eV$^2$, 0.69), and $(6.0\times10^{-11}$ eV$^2$, 0.96) [7].
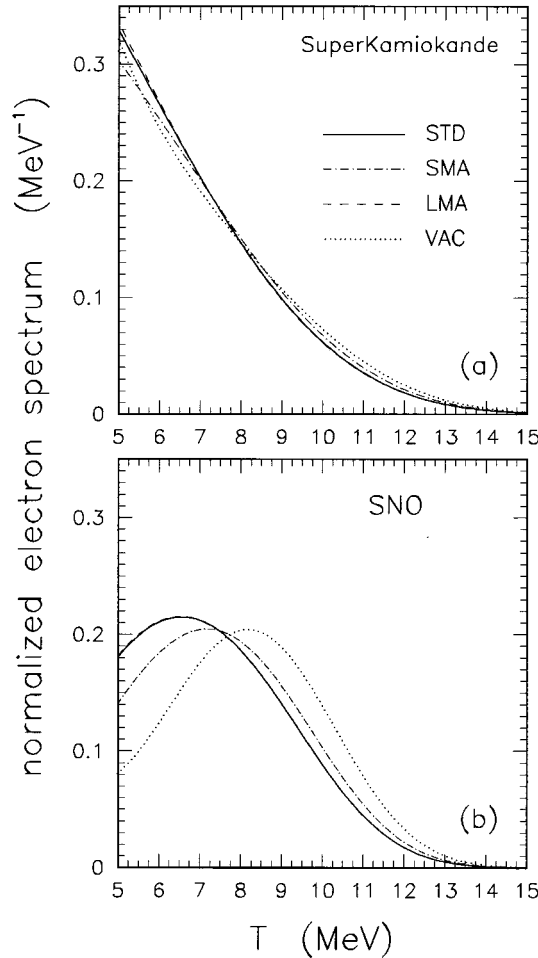
FIG. 1. Standard spectrum of the electron kinetic energy (STD, solid line) for SuperKamiokande (a) and SNO (b). Also shown are three representative spectra that apply if neutrino oscillations occur: small mixing angle MSW (SMA, dot-dashed), large mixing angle MSW (LMA, dashed), and vacuum oscillations (VAC, dotted). All spectra are normalized (area = 1). The oscillation cases correspond to best fits [7] to the results of the four pioneering solar neutrino experiments [19–22].

For the moderately small changes in the standard electron spectrum expected on the basis of many oscillation scenarios, the difference between the spectrum with and without oscillations [$f_{OSC}(T)$ and $f(T)$ respectively] can be approximated by a second order expansion in $T$ to a good approximation. Defining $\xi(T)$ as the difference between the spectrum after oscillations and the standard spectrum,

$$\xi(T) \equiv f_{OSC}(T) - f(T), \tag{6}$$

we can write

$$\xi(T) \simeq \overline{\xi}(T) \equiv f(T) \left( \beta \frac{T - \langle T \rangle_0}{\langle T \rangle_0} + \gamma \frac{T^2 - \langle T \rangle_0^2 - \sigma_0^2}{\langle T \rangle_0^2} \right), \tag{7}$$

where $\overline{\xi}(T)$ is the best quadratic approximation to $\xi(T)$.

In Eq. (7), $\beta$ and $\gamma$ are dimensionless parameters, and $\langle T \rangle_0$ and $\sigma_0^2$ are the first two moments (average and vari-

ance) of the standard distribution $f(T)$. The functional form adopted in Eq. (7) ensures that $\int dT \overline{\xi}(T) = 0$ and therefore preserves the normalization.

Within the $\mathcal{O}(T^2)$ approximation, the spectral deformations represent a two-parameter family of functions, which can be labeled either by the two parameters $(\beta, \gamma)$ or by the *deviations* and of the first two moments of the new distribution from their standard values, $\langle T \rangle_0$ and $\sigma_0^2$, through the correspondence

$$\langle T \rangle - \langle T \rangle_0 \simeq \int dT f(T) \overline{\xi}(T; \beta, \gamma) T, \tag{8}$$

$$\sigma^2 - \sigma_0^2 \simeq \int dT f(T) \overline{\xi}(T; \beta, \gamma) T^2. \tag{9}$$

It is preferable to determine the deviations of the spectral moments instead of fitting the $(\beta, \gamma)$ parameters, because the moments are well defined independently of the functional form of the shape deformation and of the order of its expansion in powers of $T$. Additional experimental information (if any) on the third or higher moments could in principle overconstrain this determination, but is not essential in the two-parameter approximation of Eq. (7).

The MSW small mixing angle solution (SMA) represents an important case in which two-moment approximation is an excellent approximation. We have checked numerically that the deviation $\xi(T) = f_{SMA}(T) - f(T)$ between the the SMA spectrum $f_{SMA}(T)$ and the STD spectrum $f(T)$ (see Fig. 1) can be parametrized accurately as indicated in Eq. (7). In the entire SMA region allowed at 95% C.L. [7] by the four pioneering solar neutrino experiments, the residuals, divided by the maximum spectral value, are small:

$$\frac{|\xi(T) - \overline{\xi}(T)|}{\max f(T)} \lesssim \begin{cases} 1\% & \text{(SuperKamiokande)}, \\ 3\% & \text{(SNO)}. \end{cases} \tag{10}$$

The large mixing angle (LMA) MSW solution is well fit by the quadratic approximation since, in any event, the LMA spectral distortions are very small (see Fig. 1).

For the best-fit vacuum oscillation solution (VAC), the residual terms of $\mathcal{O}(T^3)$ or higher in the shape deviations are as large as 10% (5%) of the maximum spectral value for SuperKamiokande (SNO). The magnitude of the residuals can be made smaller, or larger, by varying the VAC solution within the region allowed at 95% C.L. by the available data [7]. When the residuals are large, the two-moment approximation may result in a loss of information. Fortunately, precision is not crucial in the cases in which the distortions $\xi(T)$ are large. In those cases, neutrino oscillations provide a distinctive signature even with an error of the order of 10% in the large distortions.

The spectral measurements in the SuperKamiokande and SNO experiment may initially involve relatively large uncertainties. These errors will decrease as more events are accumulated and as the systematic uncertainties are better understood. If the known uncertainties are not much smaller than the changes in the spectrum, even a first-order approximation [$\gamma \simeq 0$ in Eq. (7)] can be adequate to analyze the data. The spectral deformations are then in one-to-one correspondence either with $\beta$ (see [23]), or with the deviation of $\langle T \rangle$ from

the standard value $\langle T \rangle_0$ (deviation which is proportional to $\beta$, see [8]). The use of variations of $\langle T \rangle$ to signal spectral deformations was first emphasized in [6] (see also Ref. [24]); the importance of the energy slope was first emphasized in [23].

In summary, we see that the description of the spectral deformations in terms of two parameters (i.e., the deviations of the first two moments) is a useful approach to the analysis of the SuperKamiokande and SNO measurements of the electron energy distribution. The loss of information is small for the SMA and LMA solutions. For the vacuum oscillation cases, the first two moments will also be an adequate description.

We shall show below how the neutrino oscillation parameter space can be explored by using the deviations of the first two moments from their standard values.

### III. SPECTRAL MOMENTS WITH NEUTRINO OSCILLATIONS

The calculation of the electron spectra for dense grids of values of the usual neutrino mass-mixing parameters, $\Delta m^2$ and $\sin^2 2\theta$, can be computer intensive. One has to calculate the differential neutrino cross-section, $d\sigma/dT$, smear it with the energy resolution function, and integrate the results over the $^8$B neutrino spectrum times the $\nu_e$ survival probability $P$. However, if one is interested in just the (first two) spectral moments, only one numerical integration over the neutrino energy is needed, with weight functions that are calculated once and for all. In this section we describe this fast method of calculation for the SNO and SuperKamiokande experiments. The application to vacuum and matter-enhanced neutrino oscillations will be illustrated in Sec. IV.

#### A. Moments of the SNO electron spectrum

Consider a neutrino of energy $E_\nu$ that is absorbed by deuterium, reaction (1). The cross section $\hat{\sigma}_{CC}(E_\nu)$ for producing an electron that has a measured kinetic energy greater than $T_{\min}$ is

$$\hat{\sigma}_{CC}(E_\nu) = \int_{T_{\min}} dT \int dT' R(T,T') \frac{d\sigma_{CC}(E_\nu,T')}{dT'}, \quad (11)$$

where $d\sigma/dT'$ is the differential cross section for the reaction (1) [15,8], and the energy resolution function is given in Eq. (4). The ''hat'' is intended to remind the reader that $\hat{\sigma}_{CC}$ is a smeared and reduced cross section, i.e., the electrons with *measured* energy below $T_{\min}$ are not counted.

The average value of the measured electron kinetic energy above threshold is

$$\hat{T}(E_\nu) = \hat{\sigma}_{CC}^{-1}(E_\nu) \int_{T_{\min}} dT\,T \int dT' R(T,T') \frac{d\sigma_{CC}(E_\nu,T')}{dT'}. \quad (12)$$

Analogously, the average value of the electron kinetic energy squared is

$$\hat{T}^2(E_\nu) = \hat{\sigma}_{CC}^{-1}(E_\nu) \int_{T_{\min}} dT\,T^2 \int dT' R(T,T') \frac{d\sigma_{CC}(E_\nu,T')}{dT'}. \quad (13)$$

So far we have considered a neutrino of fixed energy $E_\nu$. If we average the values of $\hat{T}(E_\nu)$ and $\hat{T}^2(E_\nu)$ over the $^8$B neutrino spectrum, $\lambda(E_\nu)$, and the $\nu_e$ survival probability, $P(E_\nu)$, we obtain

$$\langle T \rangle = \frac{\int dE_\nu \lambda(E_\nu) P(E_\nu) \hat{\sigma}_{CC}(E_\nu) \hat{T}(E_\nu)}{\int dE_\nu \lambda(E_\nu) P(E_\nu) \hat{\sigma}_{CC}(E_\nu)}, \quad (14)$$

$$\langle T^2 \rangle = \frac{\int dE_\nu \lambda(E_\nu) P(E_\nu) \hat{\sigma}_{CC}(E_\nu) \hat{T}^2(E_\nu)}{\int dE_\nu \lambda(E_\nu) P(E_\nu) \hat{\sigma}_{CC}(E_\nu)}. \quad (15)$$

The variance of the measured electron spectrum is defined as

$$\sigma^2 = \langle T^2 \rangle - \langle T \rangle^2. \quad (16)$$

The subscript ''0'' denotes ''standard'' (i.e., no oscillation) quantities:

$$\langle T \rangle_0 \equiv \langle T \rangle|_{P=1}, \quad \sigma_0^2 \equiv \sigma^2|_{P=1}. \quad (17)$$

#### B. Moments of the SuperKamiokande electron spectrum

The calculations of the spectral moments in SuperKamiokande are slightly more complicated than in SNO, since the neutrino arriving at the detector can be either a $\nu_e$ or a $\nu_\mu$, interacting with cross sections $\sigma_e$ and $\sigma_\mu$, respectively. The probabilities of these two occurrences are $P$ and $1-P$, respectively, where $P$ is the electron neutrino survival probability.

For a neutrino of energy $E_\nu$, we need to calculate the average cross section and the average electron kinetic energy for $\alpha = e, \mu$:

$$\hat{\sigma}_\alpha(E_\nu) = \int_{T_{\min}} dT \int dT' R(T,T') \frac{d\sigma_{\nu_\alpha,e}(E_\nu,T')}{dT'}, \quad (18)$$

$$\hat{T}_\alpha(E_\nu) = \hat{\sigma}_\alpha^{-1}(E_\nu) \int_{T_{\min}} dT\,T \int dT' R(T,T')$$
$$\times \frac{d\sigma_{\nu_\alpha,e}(E_\nu,T')}{dT'}. \quad (19)$$

The expression for $\hat{T}_\alpha^2(E_\nu)$ is analogous to Eq. (19) with the substitution $\hat{T}_\alpha(E_\nu) \rightarrow \hat{T}_\alpha^2(E_\nu)$.

Averaging $T$ over the neutrino spectrum, while taking into account the probabilities of $\nu_e$ and $\nu_\mu$ interactions at the detector, we obtain

$$\langle T \rangle = \frac{\int dE_\nu \lambda P \hat{\sigma}_e \hat{T}_e + \int dE_\nu \lambda (1-P) \hat{\sigma}_\mu \hat{T}_\mu}{\int dE_\nu \lambda P \hat{\sigma}_e + \int dE_\nu \lambda (1-P) \hat{\sigma}_\mu}. \quad (20)$$

For clarity, we have suppressed the $E_\nu$ dependences in Eq. (20).

The calculation of $\langle T^2 \rangle$ is analogous to Eq. (20), with the substitution $\hat{T}_\alpha \to \hat{T}_\alpha^2$. The variance $\sigma^2$ is defined as in Eq. (16).

## IV. RESULTS IN THE MASS-MIXING PLANE $(\Delta m, \sin^2 2\theta^2)$

From the discussion of the previous section, it follows that the calculation of the spectral moments in SNO and SuperKamiokande requires integrating over energy various products of the following quantities: $\lambda(E_\nu)$ ($^8$B neutrino spectrum); $\hat{\sigma}_{CC}(E_\nu)$, $\hat{T}(E_\nu)$, and $\hat{T}^2(E_\nu)$ (SNO experiment); $\hat{\sigma}_e(E_\nu)$, $\hat{T}_e(E_\nu)$, $\hat{T}_e^2(E_\nu)$, $\hat{\sigma}_\mu(E_\nu)$, $\hat{T}_\mu(E_\nu)$, and $\hat{T}_\mu^2(E_\nu)$ (SuperKamiokande experiment). These ingredients can be calculated at representative neutrino energies, given the detector parameters (Table I).

A numerical table of the above quantities can be found in [10]. The reader can find there also tables of the last ingredient needed to calculate $\langle T \rangle$ and $\sigma^2$, namely the oscillation probability $P(E_\nu)$, for the best-fit cases SMA, LMA, VAC shown in Fig. 1. Anyone wishing to evaluate the sensitivity of SuperKamiokande or SNO to some neutrino model not considered in this paper (e.g., resonant magnetic transitions, neutrino decay, violation of the equivalence principle, or exotic transitions [25]) can use the data and software in [10].

We have calculated the values of the spectral moments $\langle T \rangle$ and $\sigma^2$ for continuous ranges of the neutrino mass-mixing parameters for two-flavor oscillations. In particular, we have considered the rectangle $(\sin^2 2\theta, \Delta m^2/eV^2)$ $\in [10^{-4}, 1] \otimes [10^{-9}, 10^{-3}]$, which is relevant to MSW oscillations, and the rectangle $(\sin^2 2\theta, \Delta m^2/eV^2)$ $\in [0.4, 1] \otimes [3 \times 10^{-11}, 2 \times 10^{-10}]$, which is relevant to vacuum neutrino oscillations.

Figure 2 shows the calculated results for the SuperKamiokande experiment and Fig. 3 gives the results for the SNO experiment.

Figures 2(a) and 2(b) show the fractional differences (%) in the first two moments of the SuperKamiokande electron spectrum, $(\langle T \rangle - \langle T \rangle_0)/\langle T \rangle_0$ and $(\sigma^2 - \sigma_0^2)/\sigma_0^2$, for MSW neutrino oscillations. Superposed are the regions allowed at 95% C.L. by current fits to solar neutrino data [7] (shaded), with thick dots marking the best-fit points.

The deviations of the moments are larger in two characteristic regions, corresponding to the adiabatic MSW branch (horizontal region), and nonadiabatic MSW branch (slanted region). In the adiabatic branch, there is a strong suppression of the high-energy part of the $^8$B neutrino spectrum. Therefore the mean value of the electron energy also decreases, until there are very few electrons above the experimental threshold energy $T_{min}$ (5 MeV nominal value). The variance is also reduced by the combination of the depletion of the high energies by oscillations and the threshold cut. The fractional spectral variations are so large that part of the adiabatic branch is already excluded by the ''low statistics'' electron spectrum measurements at Kamiokande [26]. For the nonadiabatic branch (relevant for the small mixing angle solution) the low-energy part of the $^8$B neutrino spectrum is suppressed, so that both $\langle T \rangle$ and $\sigma^2$ are shifted towards

higher values. The changes in the electron spectrum are typically smaller [27] than in the adiabatic region. In the large mixing angle region, the suppression of the $^8$B neutrino spectrum is almost uniform in the energy range of interest and there are no significant deviations of the moments from their standard values.

Figures 2(c) and 2(d) show the fractional differences in the first two moments of the SuperKamiokande electron spectrum for vacuum neutrino oscillations. Also in this case there are two regions where the moments are positively or negatively shifted, corresponding to the suppression of low-energy and high-energy $^8$B neutrinos. In passing from one region to another, there are also cases in which the two moment deviations have opposite sign. These intermediate cases correspond roughly to a strong suppression of the peak of the $^8$B neutrino spectrum, and thus a secondary signature should be a low rate of events. The variations of the moments can be very strong for large values of the mixing angles. Asymptotically, they become zero for $\Delta m^2 \to \infty$ (averaged fast oscillations, uniform suppression), and for $\Delta m^2 \to 0$ or $\sin^2 2\theta \to 0$ (no oscillation).

Figures 3(a)–3(c) are analogous to Figs. 2(a)–2(c), but refer to the SNO experiment. In general, the deviations of the moments are larger than in SuperKamiokande, since the final state electrons from $\nu$-$d$ absorption are more closely correlated with the original neutrino energies than the electrons from $\nu$-$e$ scattering, and thus are more sensitive to oscillations of the parent neutrinos. We will recall this point in Sec. VI.

Figures analogous to Figs. 2(a) and 3(a) were first reported in [6]. In [6], the energy resolution function was not included, and the electron energy spectrum in $\nu$-$d$ absorption processes was approximated by a Dirac delta at any given neutrino energy (which is not a sufficient approximation, see the discussion in [8]). Alternative methods for analyzing electron spectra have been proposed in [23,28].

## V. ERROR EVALUATION

In order to test the null hypothesis of no oscillations, we need to compare the theoretical spectral moment deviations shown in Figs. 2 and 3 with realistic error estimates for $\langle T \rangle_0$ and $\sigma_0^2$.

Table II lists the standard values of the first two moments, $\langle T \rangle_0$ and $\sigma_0^2$. We will now estimate the errors affecting these values by varying the input ingredients of our calculations. A more realistic assessment of the uncertainties will be possible after the SuperKamiokande and SNO experiments have reported on detector performances.

Table III shows a preliminary assessment of the error budget for SuperKamiokande and SNO. In Table III, the errors due to the energy resolution width and energy scale are obtained by varying the parameters $\Delta_{10}$ and $\delta$ within the $1\sigma$ limits given in Table I. The error due to the $^8$B neutrino spectrum is obtained by repeating the calculation with the $\pm 3\sigma$ $^8$B spectra, $\lambda^+$ and $\lambda^-$ [16], and dividing the total spread by six. The cross section uncertainty for the SNO predictions has been estimated by comparing the values obtained with the Kubodera-Nozawa cross section [15] (default) and with the Ellis-Bahcall [29,8] cross section for the $\nu$-$d$ CC reaction. For SuperKamiokande, the $\nu$-$e$ cross sec-
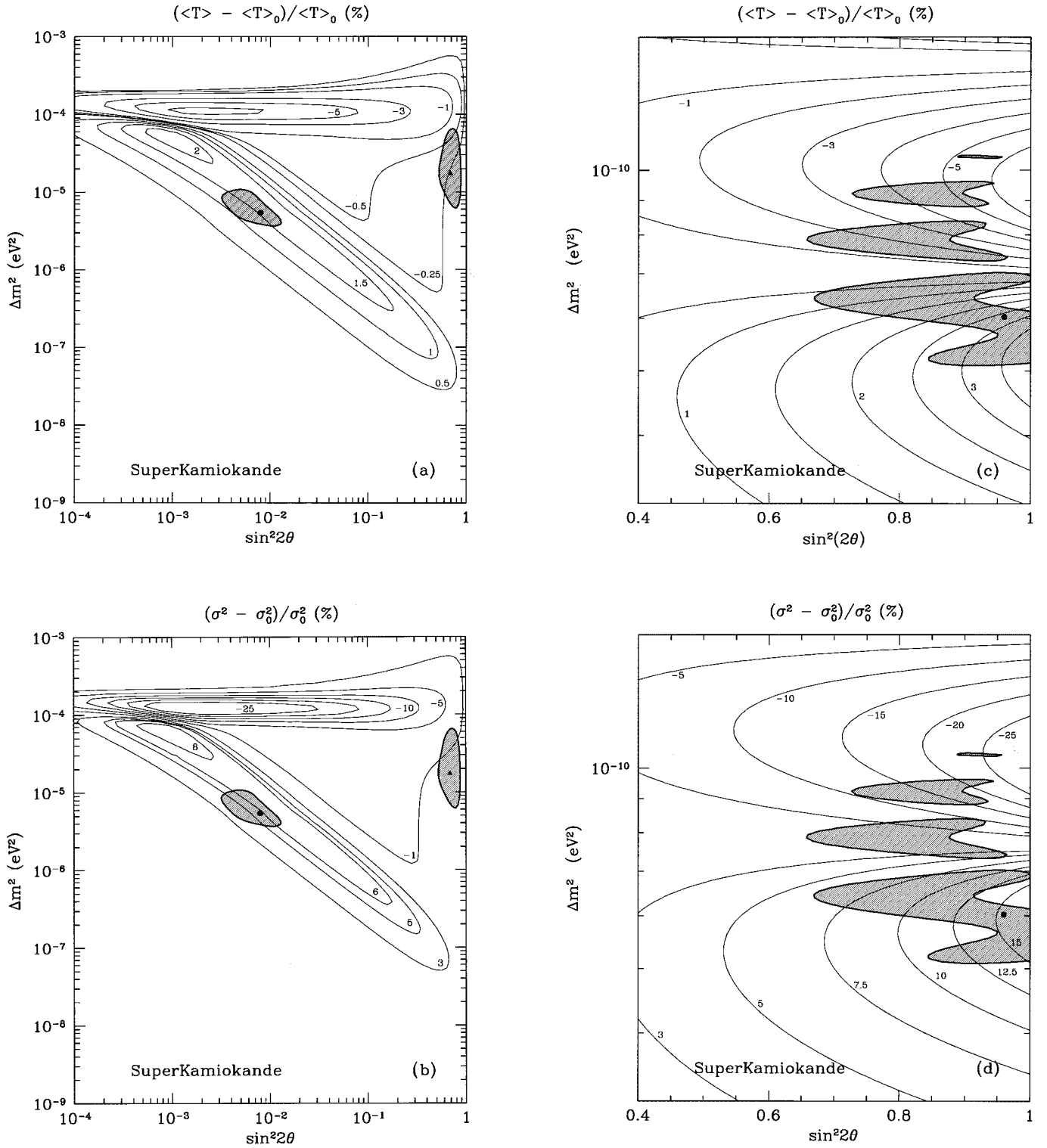
FIG. 2. SuperKamiokande experiment: fractional deviations (%) of the moments of the electron energy spectrum caused by two-flavor neutrino oscillations. The results are shown in the mass-mixing plane ($\sin^2 2\theta, \Delta m^2$). The shaded regions are favored by current solar neutrino experiments at 95% C.L. [7], with best-fit points marked by a dot. (a) Deviation of $\langle T \rangle$, MSW oscillations. (b) Deviation of $\sigma^2$, MSW oscillations. (c) Deviation of $\langle T \rangle$, vacuum oscillations. (d) Deviation of $\sigma^2$, vacuum oscillations.

tion is known to first order in the radiative corrections [12]. The first order contributions (included by default) alter $\langle T \rangle$ and $\sigma^2$ by 0.1% and 0.4% with respect to the tree-level cross section [30]. The contributions due to second and higher order corrections are expected to be smaller by a factor of

order 1/137 and can thus be neglected. The statistical errors are calculated for a representative case of $N = 5000$ collected events, which corresponds roughly to 1–2 years of operation, depending on the absolute $^8$B neutrino flux and the oscillation scenario. The error of $\langle T \rangle$ is given by $\sqrt{\sigma^2/N}$. The error

$(<T> - <T>_0)/<T>_0$ (%)

$(<T> - <T>_0)/<T>_0$ (%)

$(\sigma^2 - \sigma_0^2)/\sigma_0^2$ (%)

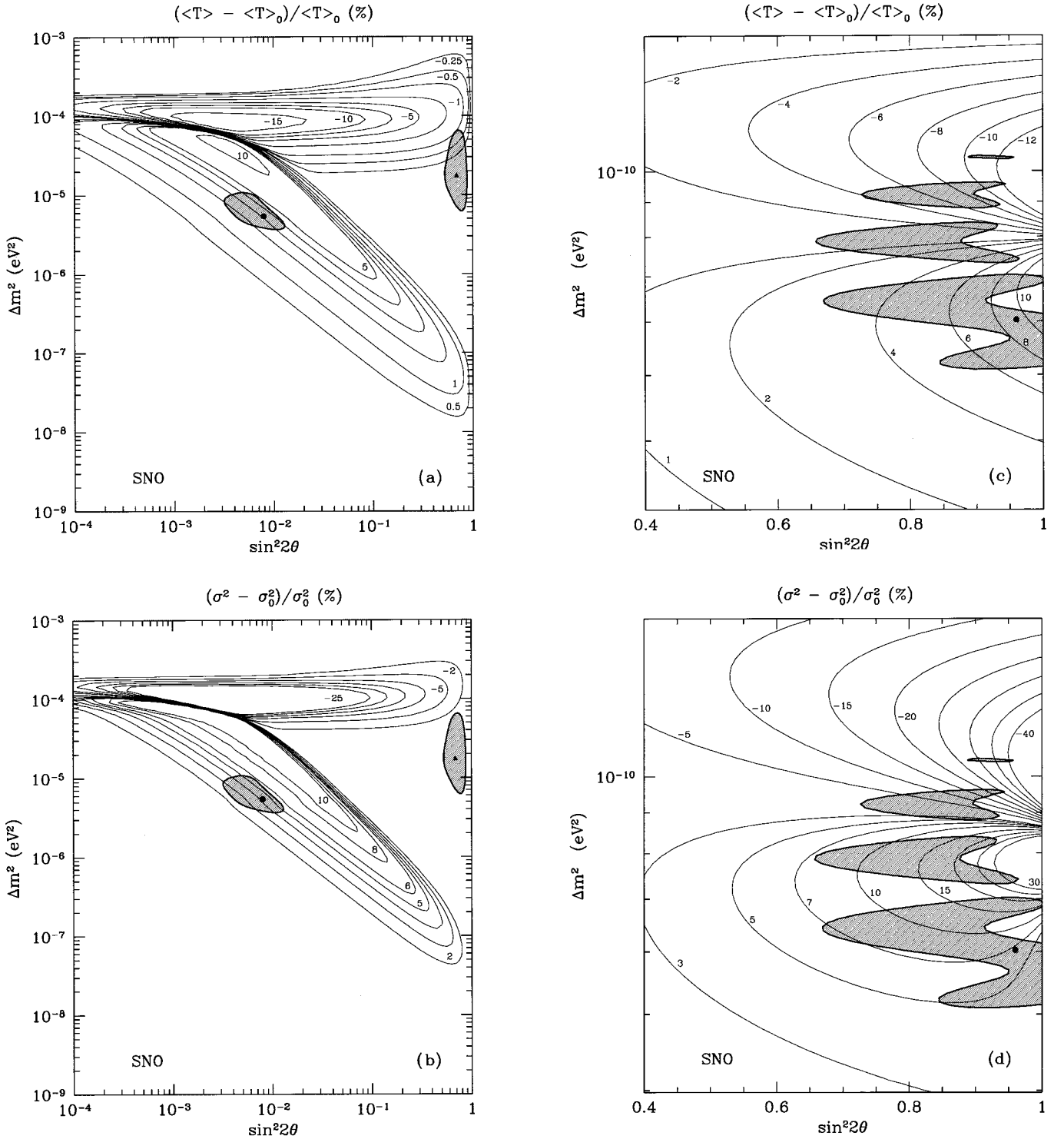$(\sigma^2 - \sigma_0^2)/\sigma_0^2$ (%)

FIG. 3. SNO experiment: fractional deviations (%) of the moments of the electron energy spectrum caused by two-flavor neutrino oscillations. The results are shown in the mass-mixing plane ($\sin^2 2\theta, \Delta m^2$). The shaded regions are favored by current solar neutrino experiments at 95% C.L. [7], with best-fit points marked by a dot. (a) Deviation of $\langle T \rangle$, MSW oscillations. (b) Deviation of $\sigma^2$, MSW oscillations. (c) Deviation of $\langle T \rangle$, vacuum oscillations. (d) Deviation of $\sigma^2$, vacuum oscillations.

of $\sigma^2$ is given by $\sqrt{[\mu_4 - (\sigma^2)^2]/N}$ [31], where $\mu_4$ is the fourth moment of the spectrum, $\mu_4 = \langle (T - \langle T \rangle)^4 \rangle$. As stated earlier, we have not included uncertainties due to the backgrounds; these uncertainties may be important.

Let us consider the error correlations in Table III. The correlation between the errors on $\langle T \rangle_0$ and $\sigma_0^2$ induced by the

uncertainties in the energy resolution width $\Delta_{10}$ (see Table I) is equal to one in modulus, since both errors depend on the same parameter ($\Delta_{10}$). The sign of the correlation is $+$ because any small positive shift in $\langle T \rangle$ tends to make the low-energy part of the electron spectrum wider (above threshold) and thus increases $\sigma^2$. For similar reasons, the errors induced

TABLE III. Estimated $1\sigma$ uncertainties ($\Delta$) of the standard moments $\langle T\rangle_0$ and $\sigma_0^2$, and their correlations ($\rho$). Possible background effects are ignored.

| | SuperKamiokande | | | SNO | | |
|---|---|---|---|---|---|---|
| $1\sigma$ uncertainties | $\Delta\langle T\rangle_0$ (MeV) | $\Delta\sigma_0^2$ (MeV$^2$) | $\rho$ | $\Delta\langle T\rangle_0$ (MeV) | $\Delta\sigma_0^2$ (MeV$^2$) | $\rho$ |
| Energy resolution width | 0.004 | 0.02 | $+1$ | 0.024 | 0.10 | $+1$ |
| Energy scale | 0.025 | 0.06 | $+1$ | 0.052 | 0.08 | $+1$ |
| $^8$B neutrino spectrum | 0.016 | 0.04 | $+1$ | 0.029 | 0.05 | $+1$ |
| Cross section | $\sim 0$ | $\sim 0$ | $\sim 0$ | 0.011 | 0.01 | $\sim 0$ |
| Statistics ($N=5000$) | 0.026 | 0.08 | $+0.63$ | 0.025 | 0.06 | $+0.45$ |
| Total $1\sigma$ error | 0.040 | 0.11 | $+0.80$ | 0.070 | 0.15 | $+0.83$ |
| Total fractional error | 0.54% | 3.2% | $+0.80$ | 0.91% | 4.9% | $+0.83$ |

by the energy scale uncertainty, as well as by the neutrino spectrum uncertainties, have correlation $+1$. The cross-section errors are small (negligible for SuperKamiokande) and their correlation can be ignored. The correlation of the statistical errors is $\rho=\mu_3/[\sqrt{\sigma^2}\sqrt{\mu_4-(\sigma^2)^2}]$ [31], where $\mu_3$ is the third moment of the electron energy spectrum.

## VI. ISO-SIGMA CONTOURS FOR SUPERKAMIOKANDE AND SNO

In this section we illustrate the diagnostic power of SuperKamiokande and SNO to reveal possible new physics by measuring electron energy spectra.

Figure 4 shows contours of equal standard deviations ($n$-sigma ellipses)[4] in the plane of the $\langle T\rangle$ and $\sigma^2$ deviations that were obtained with the help of Table III. The contours are centered around the standard expectations (STD). Also shown are the representative best-fit points VAC and SMA. The point LMA is very close to STD and is not shown.

The cross centered at the SMA best-fit point indicates the solution space allowed at 95% C.L. [7] by the solar neutrino data published so far [see Figs. 2(a), 2(b), 3(a), and 3(b)]. The deviations in $\langle T\rangle$ and $\sigma^2$ for the SMA solution are confined in a relatively small range. For vacuum oscillations, the range of deviations spanned by the whole region allowed at 95% C.L. by present data [Figs. 2(c), 2(d), 3(c), 3(d)] is much larger and is not indicated in Fig. 4. The statistical significance of the separation between the SMA and STD points in Fig. 4 is dominated by the fractional shift in $\langle T\rangle$ for both SuperKamiokande and SNO. This is not surprising, since the SMA neutrino survival probability increases almost linearly with energy for $E_\nu\gtrsim 5$ MeV; this increase induces deformations of the electron spectra that are nearly linear in $T$ and are well represented by a shift in $\langle T\rangle$, as discussed in Sec. II (see also [8]).

The best-fit small mixing angle solution is separated by $\gtrsim 3\sigma$ from the standard solution for both SuperKamiokande and SNO (see Fig. 4). The discriminatory power of the two experiments appears to be comparable for the SMA solution. The estimated total fractional errors of $\langle T\rangle$ and $\sigma^2$ in Su-

perKamiokande are about a factor of two smaller than in SNO (see Table III). However, the purely CC interaction in SNO [Eq. (1)] is a more sensitive probe of neutrino oscillations than a linear combination of CC and NC interactions,
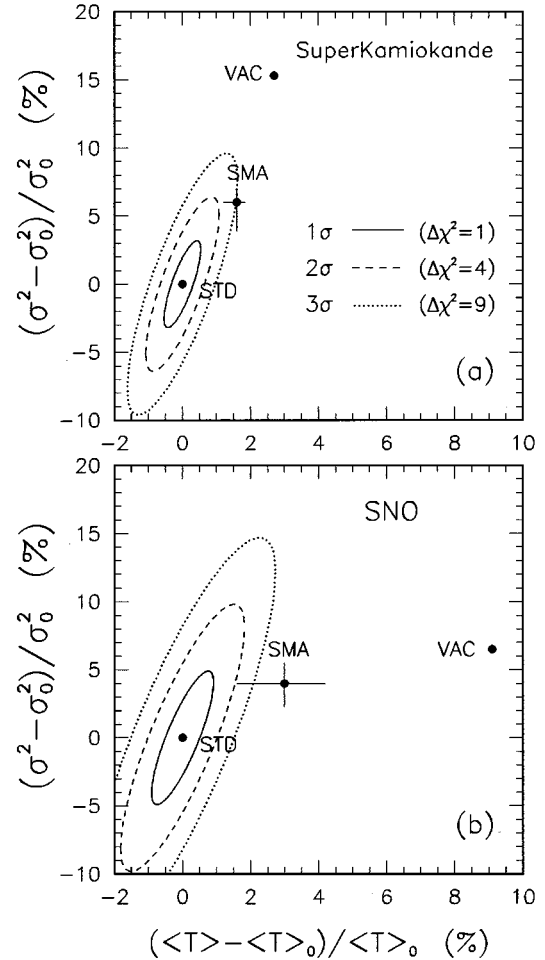


FIG. 4. Iso-sigma contours in the plane of the fractional deviations of the first two spectral moments. Labels are as in Fig. 1. (a) SuperKamiokande experiment. (b) SNO experiment. The SMA solution can be distiguished at $\gtrsim 3\sigma$ from the standard (STD) case by both experiments. The crosses allow for variations of the SMA solution within the region favored at 95% C.L. by the current experiments. See the text for details.

---

[4]The ''number of sigmas'' $n$ is defined as $n=\sqrt{\chi^2}$. The probability content of the error ellipses is given by the $\chi^2$ distribution for two degrees of freedom [32].

TABLE IV. The correlation matrix of the total errors affecting the measurements of $\langle T \rangle_0$ and $\sigma_0^2$ at SuperKamiokande (SK) and SNO. The correlations between the SK and SNO entries arise from the common uncertainty in the $^8$B neutrino spectral shape.

| | $\langle T \rangle_0$ (SK) | $\sigma_0^2$ (SK) | $\langle T \rangle_0$ (SNO) | $\sigma_0^2$ (SNO) |
|---|---|---|---|---|
| $\langle T \rangle_0$ (SK) | 1.00 | 0.80 | 0.17 | 0.13 |
| $\sigma_0^2$ (SK) | | 1.00 | 0.15 | 0.12 |
| $\langle T \rangle_0$ (SNO) | | | 1.00 | 0.83 |
| $\sigma_0^2$ (SNO) | | | | 1.00 |

as observed in SuperKamiokande [Eqs. (2) and (3)].[5] Moreover, the final electron energy in the $\nu_e + d \rightarrow p + p + e^-$ absorption interaction is more closely correlated with the initial neutrino energy than in $\nu + e^- \rightarrow \nu' + e^-$ scattering. The SuperKamiokande detector (according to the available information about the likely performances of the detectors) may compensate a lower sensitivity to neutrino oscillations with a more precise control of the systematics related to the electron energy measurement.

How do the above results depend upon the energy threshold? We have verified by detailed calculations that the statistical significance of the SMA deviations in Figs. 4(a) and 4(b) decreases by about $0.6\sigma$ per 1 MeV increase in the energy threshold $T_{\min}$. These results are valid for both the SNO and the SuperKamiokande detectors and include calculations for thresholds of 5, 6, and 7 MeV.

Although SuperKamiokande and SNO are calculated to be about equally sensitive to the SMA solution, different new physics scenarios may be more easily tested by one or the other of the two experiments. For instance, the SNO experiment appears to be more sensitive than SuperKamiokande to the best-fit vacuum solution (VAC point in Fig. 4).

When both the SuperKamiokande and the SNO electron spectra have been measured, it will be important to estimate the correlation of their errors. In fact, the uncertanties affecting the spectra measured in these two different experiments are all independent of each other except for the uncertainty in the shape of the input neutrino spectrum [16], which is common to both experiments. The uncertainties in the neutrino spectrum will induce a correlation between the errors in the spectrum shapes measured by SNO and SuperKamiokande. For the spectral moments and the detector parameters used in this work, the correlation matrix between the total errors of SuperKamiokande and SNO is shown in Table IV. The submatrix that links SNO and SuperKamiokande quantities has relatively small entries, $\rho = 0.12-0.17$, indicating that the ''cross talk'' induced by the common neutrino spectrum sys-

tematics is relatively unimportant. However, this relatively small error correlation may increase or decrease for more realistic detector parameters and experimental uncertainties, that will be determined after the experiments have been operating for some time.

## VII. SUMMARY

In this paper we propose that the electron energy spectra that will be measured in the SuperKamiokande and SNO experiments be characterized by their first two moments, namely the average electron kinetic energy $\langle T \rangle$ and the variance of the energy distribution $\sigma^2$.

We have shown in Sec. II C that the two-moment approximation is accurate for the MSW solutions favored by the four pioneering solar neutrino experiments [19–22] and is a good approximation to the distortions induced by vacuum oscillations except for those cases in which the distortion is very large and obvious.

We have presented in Tables II and III the standard values, and estimated uncertainties, of $\langle T \rangle$ and $\sigma^2$ in the absence of oscillations. We have also presented in Figs. 2 and 3 the fractional deviations of the two spectral moments induced by neutrino oscillations in the whole neutrino mass-mixing parameter space relevant to MSW or vacuum two-flavor oscillations. The deviations from the standard values can be greater than $3\sigma$, as shown in Fig. 4, in a large region of the neutrino parameter space, part of which is currently favored by the published results of the four pioneering solar neutrino experiments. The statistical significance of the SMA deviations for both SNO and SuperKamiokande decrease by about $0.6\sigma$ per MeV for energy thresholds in the range between 5 and 7 MeV.

*Note added.* After this paper was completed, H. Sobel suggested we investigate what would be the effect of reducing the uncertainty in the energy scale $\delta$ in the SuperKamiokande experiment from 100 keV to 50 keV. We find that if $\delta$ is reduced to 50 keV the total uncertainty in both moments is reduced by about 15% (5000 events assumed) and the significance of the SMA signal is increased by about $0.5\sigma$ (to about $3.5\sigma$). The uncertainty in the $^8$B neutrino spectrum would be the dominant systematic uncertainty (excluding background effects) if the energy scale error were as small as 50 keV.

---

[5]In practice, the separation of CC and NC events in SNO will be affected by experimental uncertainties. We have ignored this misidentification error as well as all the backgrounds.

---

[1] Y. Totsuka, in *Physics and Astrophysics of Neutrinos*, edited by M. Fukugita and A. Suzuki (Springer-Verlag, Tokyo, 1994), p. 625; A. B. McDonald, in *TAUP '95*, Proceedings of the 4th International Workshop on Theoretical and Phenom-enological Aspects of Underground Physics, Toledo, Spain, edited by A. Morales, J. Morales, and J. A. Villar [Nucl. Phys. B (Proc. Suppl.) **48**, 357 (1996)]; C. Rubbia, *ibid.*, p. 172.

[2] J. N. Bahcall, Phys. Rev. D **44**, 1644 (1991).

[3] Y. Totsuka, in *TAUP '95* [1], p. 547; A. Suzuki, in *Physics and Astrophysics of Neutrinos* [1], p. 414.

[4] SNO Collaboration, G. T. Ewan *et al.*, ''Sudbury Neutrino Observatory Proposal,'' Report No. SNO-87-12, 1987 (unpublished); ''Scientific and Technical Description of the Mark II SNO Detector,'' edited by E. W. Beier and D. Sinclair, Queen's University Report No. SNO-89-15, 1989 (unpublished); A. B. McDonald, in *Proceedings of the 9th Lake Louise Winter Institute*, edited by A. Astbury *et al.* (World Scientific, Singapore, 1994), p. 1.

[5] H. H. Chen, Phys. Rev. Lett. **55**, 1534 (1985).

[6] G. Fiorentini, M. Lissia, G. Mezzorani, M. Moretti, and D. Vignaud, Phys. Rev. D **49**, 6298 (1994).

[7] J. N. Bahcall and P. I. Krastev, Phys. Rev. D **53**, 4211 (1996).

[8] J. N. Bahcall and E. Lisi, Phys. Rev. D **54**, 5417 (1996).

[9] Current information on the status of the SNO experiment can be retrieved from the following URL: http://snodaq.phy.queensu.ca/SNO/sno.html.

[10] FORTRAN codes for the calculation of the differential $\nu$-$d$ and $\nu$-$e$ cross sections, and other software and data related to solar neutrinos are available at the URL: http://www.sns.ias.edu/~jnb/ (see ''Neutrino Export Software and Data'').

[11] Current information on the status of the SuperKamiokande experiment can be retrieved from the following URL's: http://www-sk.icrr.u-tokyo.ac.jp/ and http://www.ps.uci.edu/~superk/.

[12] J. N. Bahcall, M. Kamionkowsky, and A. Sirlin, Phys. Rev. D **51**, 6146 (1995).

[13] Y. Totsuka and Y. Suzuki, private communication.

[14] E. W. Beier, private communication.

[15] K. Kubodera and S. Nozawa, Int. J. Mod. Phys. E **3**, 101 (1994).

[16] J. N. Bahcall, E. Lisi, D. E. Alburger, L. De Braeckeleer, S. J. Freedman, and J. Napolitano, Phys. Rev. C **54**, 411 (1996).

[17] V. N. Gribov and B. M Pontecorvo, Phys. Lett. **28B**, 493 (1969); J. N. Bahcall and S. C. Frautschi, *ibid.* **29B**, 623 (1969); S. L. Glashow and L. M. Krauss, Phys. Lett. B **190**, 199 (1987).

[18] L. Wolfenstein, Phys. Rev. D **17**, 2369 (1978); S. P. Mikheyev and A. Yu. Smirnov, Yad. Fiz. **42**, 1441 (1985) [Sov. J. Nucl. Phys. **42**, 913 (1986)].

[19] R. Davis, Prog. Part. Nucl. Phys. **32**, 13 (1994); B. T. Cleveland *et al.*, in *Neutrino '94*, Proceedings of th 16th International Conference on Neutrino Physics and Astrophysics, Eilat, Israel, edited by A. Dar, G. Eilam, and M. Gronau [Nucl. Phys. B (Proc. Suppl.) **31**, 47 (1995)].

[20] GALLEX Collaboration, P. Anselmann *et al.*, Phys. Lett. B **357**, 237 (1995).

[21] SAGE Collaboration, J. S. Nico *et al.*, in *ICHEP '94*, Proceedings of the 27th International Conference on High Energy Physics, Glasgow, Scotland, edited by P. J. Bussey and I. Knowles (IOP, Bristol, 1995), Vol. II, p. 965; J. N. Abdurashitov *et al.*, Phys. Lett. B **328**, 234 (1994).

[22] Kamiokande Collaboration, Y. Suzuki *et al.*, in *Neutrino '94* [19], p. 54; K. S. Hirata *et al.*, Phys. Rev. D **44**, 2241 (1991); **45**, 2170(E) (1992).

[23] W. Kwong and S. P. Rosen, Phys. Rev. D **51**, 6159 (1995); see also Phys. Rev. Lett. **68**, 748 (1992).

[24] Z. G. Berezhiani and A. Rossi, Phys. Rev. D **51**, 529 (1995).

[25] See the papers from ''Physics Beyond the Standard Model'' reprinted in *Solar Neutrinos, The First Thirty Years*, edited by R. Davis, Jr., P. Parker, A. Yu. Smirnov, and R. Ulrich, Frontiers in Physics (Addison-Wesley, Reading, MA, 1994), Vol. 92.

[26] KamioKande Collaboration, K. S. Hirata *et al.*, Phys. Rev. Lett. **65**, 1301 (1990).

[27] J. N. Bahcall and H. A. Bethe, Phys. Rev. Lett. **65**, 2233 (1990).

[28] P. I. Krastev and A. Yu. Smirnov, Phys. Lett. B **338**, 282 (1994); P. I. Krastev and S. T. Petcov, Nucl. Phys. **B449**, 605 (1995).

[29] S. D. Ellis and J. N. Bahcall, Nucl. Phys. **A114**, 636 (1968).

[30] J. N. Bahcall, *Neutrino Astrophysics* (Cambridge University Press, Cambridge, 1989); G. 't Hooft, Phys. Lett. **37B**, 195 (1971).

[31] M. G. Kendall and A. Stuart, *The Advanced Theory of Statistics* (Hafner, New York, 1969), Vol. I.

[32] Particle Data Group, L. Montanet *et al.*, Phys. Rev. D **50**, 1173 (1994).